Structure of gold atoms on stoichiometric and defective ceria surfaces

Changjun Zhang,[1] Angelos Michaelides,[2] David A. King,[1] and Stephen J. Jenkins[1,a)]
[1]*Department of Chemistry, University of Cambridge, Lensfield Road, Cambridge CB2 1EW, United Kingdom*
[2]*London Centre for Nanotechnology and Department of Chemistry, Materials Simulation Laboratory, University College London, London WC1H 0AH, United Kingdom*

(Received 25 May 2008; accepted 7 October 2008; published online 21 November 2008)

Within the framework of the GGA+U implementation of density functional theory, we investigate atomistic and electronic structures of Au adsorbed on the stoichiometric and the defective $CeO_2\{111\}$ surfaces, in the latter of which either O or Ce vacancies are presented. We show that on the stoichiometric surface, the most stable adsorption site of Au is not on the top of the outermost O atoms, as previously suggested, but on a bridgelike site in which the Au directly binds to two O atoms. We suggest that on both sites, the original empty Ce 4f states near the Fermi level facilitate the oxidation of the Au; the preference of the Au for being on the bridgelike site is due to the larger O 2p-d(Au) mixing, accompanied by more significant electron redistributions. On the reduced surface with O vacancies, the most stable adsorption site of Au is near the vacancy position. Unlike that on the stoichiometric surface, strong ionic bonding character exists between Au and Ce, as the former becomes $Au^{\delta-}$ due to the occupation of the 6s(Au) orbitals. Upon substitution for one of the Ce atoms in the lattice, the Au possesses a much stronger positive charge than that in other cases. We find that although Au is strongly bonded when it is at the Ce vacancy site, the overall binding (i.e., with the Ce vacancy formation energy being taken into account) is weaker than that for Au adsorbed at the stoichiometric surface. © *2008 American Institute of Physics*.
[DOI: 10.1063/1.3009629]

I. INTRODUCTION

Ceria-supported gold catalysts have recently attracted much research interest, primarily due to the excellent activity of the catalysts reported for the low-temperature water-gas shift (WGS) reaction, which is a crucial step in many applications such as the production of hydrogen for fuel cells.[1] Despite extensive studies, some fundamental issues remain disputed such as the catalytic roles of the gold nanoparticles and the ceria support, and the relative importance of different WGS reaction mechanisms.[2] In addressing these issues, detailed knowledge of the structure of gold on ceria is of great importance.

The structure of gold on ceria, especially the oxidation state of Au, has been studied experimentally, but conclusions vary widely. By investigating both the fresh and leached samples of Au/CeO_2, Fu *et al.*[1] found that after the metallic Au was removed, the system catalyzed the WGS reaction just as well as did the original catalyst. They therefore suggested that the metallic Au nanoparticles do not participate in the WGS reaction, and that the catalytic activity of the system is due to Au cations. In contrast, Tabakova *et al.*[3] proposed different oxidation states of Au. By using CO adsorption as a probe of the nature of the Au/CeO_2 catalysts, they applied Fourier transform infrared spectroscopy on the systems to observe bands at 2060 and at 2100 cm^{-1}, which were assigned to the CO adsorbed on the $Au^{\delta-}$ sites and the metallic Au^0 sites, respectively. By using EXAFS and XANES, Tibiletti *et al.*[4] also studied the structure of Au on the CeO_2 support. They suggested that Au in the fresh catalysts can be in the form of Au cations; under WGS reaction conditions, however, they believed that the active site comprises metallic Au clusters, containing about 50 atoms, in close contact with the oxide support. The active site involving small Au clusters has also been proposed by Rodriguez *et al.*[5,6] who suggested from *in situ* time-resolved x-ray diffraction and adsorption spectroscopy data that cationic Au are not the key sites responsible for the WGS reactivity. Furthermore, they showed that the WGS activity of Au/CeO_{2-x} is more active than Au/CeO_2, and Au clusters interacting with O vacancies of ceria support constitute the chemically active phase.

There are several theoretical studies concerning $Au/CeO_2\{111\}$ systems in the literature. By using density functional theory (DFT), Liu *et al.*[7] investigated a single Au atom and a small cluster of four Au atoms on ceria, concluding that $Au^{\delta+}$ is the catalytic species and that a combination of several $Au^{\delta+}$ in the vicinity of an O vacancy can facilitate the WGS reaction. Tibiletti *et al.*[4] calculated a single Au atom on ceria surfaces with DFT and found that Au at a Ce vacancy is very stable; they further suggested that the Au cluster is bound to the ceria surface via the Au atom at the Ce vacancy. Shapovalov *et al.*[8] also used DFT to study CO oxidation on a $Au_xCe_{1-x}O_2$ model, in which a Au atom substitutes one of the Ce atoms in the ceria lattice, and they showed that Au can facilitate O vacancy formation.

Theoretical description of ceria-supported gold systems often faces the following two issues. First, there exist various Au structures proposed in experiment, and conclusions could be highly sensitive to the Au models chosen in the calcula-

a)Author to whom correspondence should be addressed. Electronic mail: sjj24@cam.ac.uk.

tions. Thus, a systematic examination of different models is necessary.[9] Second, it is not entirely straightforward to treat the strongly correlated f electrons, in particular, in the case of reduction of Ce^{4+} to Ce^{3+}: for example, standard DFT calculations would predict a wrong metallic ground state for Ce_2O_3. This issue has recently been vigorously tackled.[10–13] It has been shown that the shortcomings of standard DFT can be overcome by the DFT+U approach, in which the introduction of the Hubbard U term modifies the intra-atomic Coulomb interaction so as to stabilize the insulating solution of Ce_2O_3. We should mention that many previous studies concerning Au/CeO_2 systems excluded the U term,[4,7,8] although in the calculations of Liu *et al.*,[7] modifications of the Broyden mixing scheme were made so that in the change of $Ce^{4+} \rightarrow Ce^{3+}$ upon the creation of an O vacancy, the broken-symmetry solutions of the Ce valency were preserved. Therefore, it remains to be seen to what extent the inclusion of a U term in DFT calculations would affect the adsorption systems. In this study, by using the DFT+U approach, we carry out a systematic study of Au adsorbed on the stoichiometric and the defective ceria surface, in the latter of which either O or Ce vacancies are presented. We concentrate here on the single Au atom adsorption on the surfaces, because of the uncertainty of the exact size and shape of typical Au clusters. We note that a very recent study has investigated similar systems to ours.[9] Unlike that study,[9] however, we investigate various possible surface sites to identify the most stable adsorption modes; we focus on changes of electronic structures upon Au adsorption, especially the behavior of the Ce 4f orbitals, which play an important role in determining the adsorption structure and energetics.

II. CALCULATIONS

The calculations were performed using the Vienna *ab initio* simulation program (VASP), a widely used plane-wave pseudopotential DFT package.[14] We chose the DFT+U methodology[15,16] in order to obtain correct electronic features of ceria systems. The physical idea behind the DFT+U approach comes from the Hubbard Hamiltonian. In the practical implementations in the VASP code, the formulation of Liechtenstein *et al.*[17] and Dudarev *et al.* was used,[18] in which the on-site two-electron integrals are expressed in terms of a single parameter, U_{eff}. This U_{eff} is defined as the difference between the spherically averaged Hubbard parameter U and the screened exchange energy parameter I, which reflect the strength of the on-site Coulomb interaction and of the exchange interaction, respectively. The DFT+U approach can be understood as the introduction of a penalty function, which disfavors noninteger occupation numbers of the on-site density matrix. In other words, the DFT+U correction acts to reduce the one-electron potential locally for the specified orbitals of the metal atoms (e.g., f orbitals of Ce), therefore reducing the hybridization with orbitals of the ligands (e.g., O atoms). As shown in previous studies,[10–13] the introduction of U_{eff} improves the description of ceria systems. In practice, however, the choice of U_{eff} value is often empirical, which is to say that the parameter is adjusted to reproduce properties known in experiments. There are a host of papers devoted to the discussion of appropriate U_{eff} values.[11,13,19–21] In this study, we set $U_{\text{eff}}=5$ eV, a common choice in studying ceria surfaces in the literature.[9,19] Consistent with previous work,[19] we have found that the degree of delocalization of the f orbitals decreases with increasing U_{eff} values: for example, $U_{\text{eff}}=3$ eV would lead to electron delocalization among all three Ce atoms in the vicinity of an O vacancy, while $U_{\text{eff}}=5$ eV would give correct results of electron localization that is rather independent of specific values of $U_{\text{eff}}>5$ eV.

The DFT solution within the DFT+U approach can be obtained either at the LDA or GGA levels, giving rise to what have been called the LDA+U and the GGA+U formulations, respectively. We have used here the GGA+U approximation with a GGA functional built from the Perdew and Zunger[22] local functional, with the spin interpolation formula of Vosko *et al.*[23] and the gradient corrections by Perdew *et al.*[24] In our calculation, the interaction between the valence electrons and the core was described with the projected augmented wave method in the implementation of Kresse and Joubert.[25] The Ce 5s, 5p, 5d, 4f, 6s electrons, the O 2s and 2p electrons, and the Au 5d, 6s and 6p electrons were treated as valence electrons. The number of plane waves is controlled by a cutoff energy, which was chosen as 500 eV, sufficient to obtain well-converged energies. For integration within the Brillouin zone, specific k-points were selected using a $4\times4\times4$ Monkhorst–Pack grid for bulk CeO_2 and a $4\times4\times2$ grid for bulk Ce_2O_3. These settings are able to generate lattice constants of 5.48 Å for bulk CeO_2 and 3.88 Å for bulk Ce_2O_3, which compare well with the experimental values (5.41 and 3.89 Å, respectively), and to reproduce the characteristic electronic features including the energy level of f states and the insulating solution of Ce_2O_3.

The {111} face of ceria, chosen in this study, features an oxygen termination of stoichiometric O–Ce–O trilayers stacked along the [111] direction and is the thermodynamically most stable surface. Two unit cells of the CeO_2{111} surface, (2×2) and (3×5), are used in our calculations. The smaller unit cell was chosen so that we can make direct comparison with previous studies. The larger (3×5) unit cell was chosen partially because the interaction of isolated Au atoms between cells needs to be examined and partially because the greater number of inequivalent atoms presented in the unit cell allows us to examine different spin distributions (i.e., different starting configurations of the spin density, and the location of the Ce^{3+}, in particular). Our surface models contain nine atomic layers (or three layers of CeO_2 units) and ~12 Å vacuum regions. In the stoichiometric cell, the top three layers of the slab were relaxed until the forces were smaller than 0.025 eV/Å while the rest of the atoms were constrained to their bulk positions, whereas in the defective cells the top six layers were allowed to relax toward the set tolerance. Monkhorst–Pack k-point meshes of $4\times4\times1$ and $3\times2\times1$ were used for the (2×2) and (3×5) cells, respectively, sufficient to obtain well-converged energies.

For reference in the later discussion, we plot in Fig. 1 the total density of states (DOS) of the stoichiometric and the reduced surfaces. In the former, the valence band is composed of predominantly O 2p; the relatively narrow unoccu-

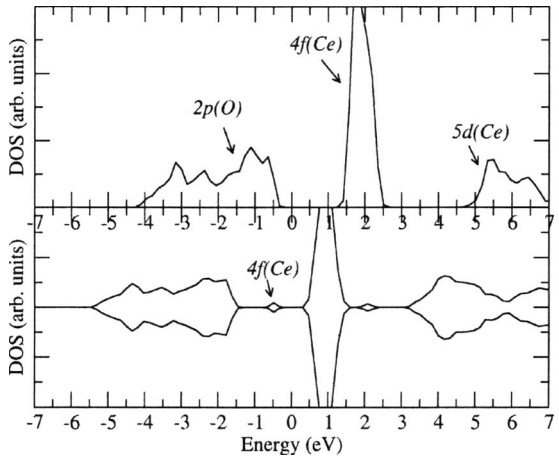

FIG. 1. The total DOS of the stoichiometric surface (top) and that of the reduced surface (bottom), in which the Fermi levels are set at zero. The DOS for the reduced surface is shown spin resolved. Characters of typical peaks are indicated by arrows.

pied band above the Fermi level (E_F) is derived from Ce $4f$; the conduction band has the main contributions from $5d$(Ce). In the latter, an occupied band of the gap states appears at below E_F, and the spins localize on the two Ce ions neighboring the O vacancy. These features are well documented in the literature.[11,19]

III. RESULTS

In the following three subsections, we present the results for Au on the stoichiometric surface, the surface with an O vacancy, and the surface with a Ce vacancy. On the stoichiometric surface, we consider various possible sites for Au adsorption and discuss electronic structures of different adsorption modes, which have not been investigated before. On the surfaces with vacancies, we consider only the adsorption at the vacancies, as other adsorption modes are much weaker; we focus on the electronic features rather than the geometrical ones.

A. Au on the stoichiometric surface

We consider the apparent high-symmetry sites and less symmetric sites, such as an initial position between an outermost O atom and an adjacent Ce atom, and an initial position between an outermost O atom and an adjacent subsurface O atom (Fig. 2). Our calculations show that Au at those less symmetrical sites is not stable and would move to the high-symmetry sites in the structural optimizations. Four distinct stable sites have been identified, which are identified as top, bridge, and hollow-O and hollow-Ce in Fig. 2. Note that the bridge site refers to a position between two surface O atoms, although not exactly on the line connecting the two, whereas the two hollow sites refer to the positions where the atoms beneath Au in the third atomic layer are O and Ce, respectively. The main structural parameters in the four adsorption configurations and the calculated adsorption energies are summarized in Table I. The adsorption energy (ΔE_a) is defined with respect to the isolated Au atom and the bare surfaces, in accord with previous studies,[4,7,9] i.e.,

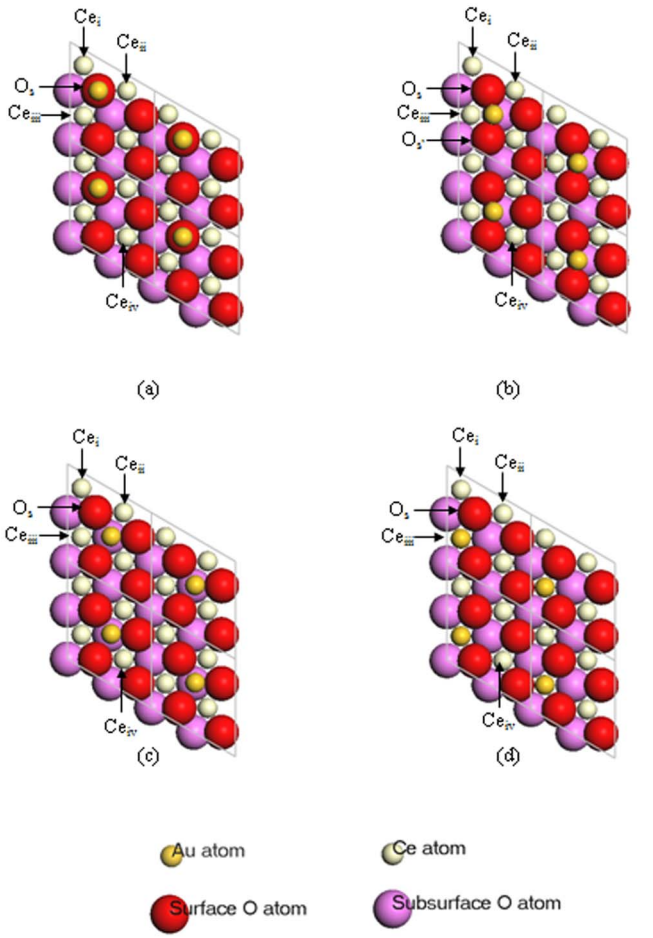

FIG. 2. (Color online) Top views of different configurations of Au adsorbed on (a) top site, (b) bridge site, (c) hollow-O, and (d) hollow-Ce site. Some Ce and O atoms are labeled.

$$\Delta E_a = E_{\text{surf}}^{\text{Au}} - E_{\text{surf}} - E_{\text{Au}}, \tag{1}$$

where the terms are self-explanatory. It can be seen clearly from Table I that the most stable adsorption site is not the top site, as suggested previously, but the bridge site, although the difference of the adsorption energies between the two sites is not large; the hollow sites are comfortably the least favorable. We should mention that the energy ordering of the Au

TABLE I. Main structural parameters and adsorption energies (ΔE_a) of Au adsorbed on different sites of the stoichiometric surface. The labeling conventions of Ce atoms and O atom are indicated in Fig. 2. Results from the large (3×5) cell are written in parentheses.

	Top	Bridge	Hollow-O	Hollow-Ce
Au–O_s (Å)	2.00 (1.98)	2.19 (2.17)	2.74	3.13
Au–Ce_i (Å)	3.82 (3.80)	⋯	⋯	⋯
Au–Ce_{ii} (Å)	3.87 (3.88)	3.35 (3.38)	3.23	⋯
Au–Ce_{iii} (Å)	3.82 (3.80)	2.87 (2.87)	3.23	⋯
Au–Ce_{iv} (Å)	⋯	3.35 (3.30)	3.23	⋯
O_s–Ce_i (Å)	2.51 (2.55)	2.61 (2.68)	2.37	2.37
O_s–Ce_{ii} (Å)	2.54 (2.58)	2.39 (2.39)	2.38	2.38
O_s–Ce_{iii} (Å)	2.51 (2.55)	2.56 (2.62)	2.38	2.38
O_s–Ce_{iv} (Å)	⋯	⋯	⋯	⋯
ΔE_a (eV)	−0.96 (−1.01)	−1.17 (−1.14)	−0.66	−0.43

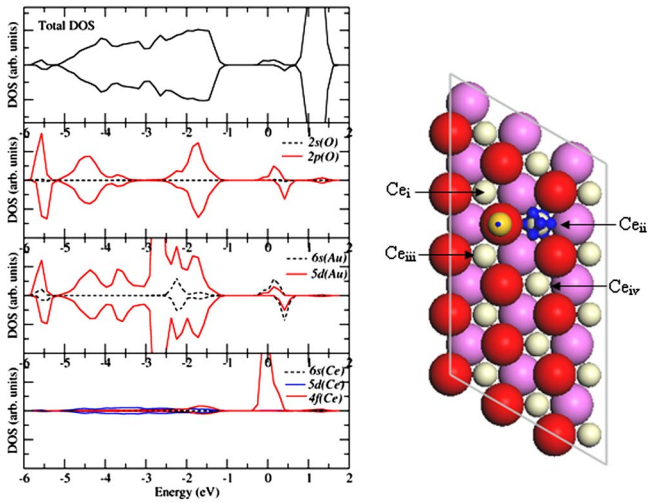

FIG. 3. (Color online) (a) The total (top panel) and atom-resolved projected DOS of the Au adsorbed on the top site, the latter of which are rescaled so that the characteristic features can be seen more clearly. The O and Ce atoms (i.e., Ce_{ii}) in the PDOS refer to those directly involved in the bonding upon Au adsorption. (b) The three-dimensional contour plot of the spin density [dark areas around atoms (blue areas)] of the system. For clarity, results from the (3×5) cell are shown.

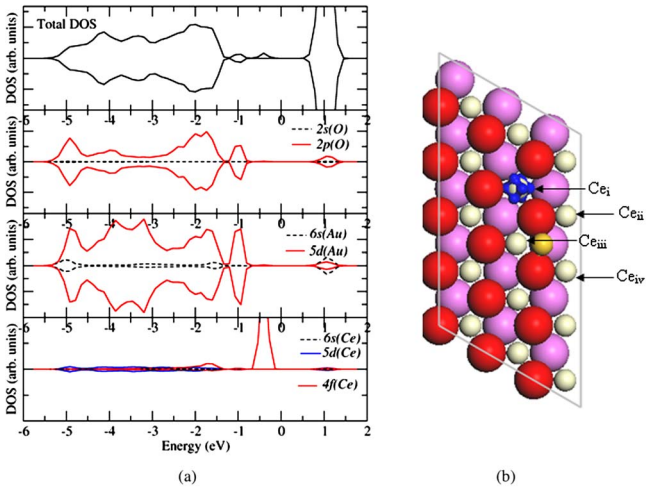

FIG. 4. (Color online) (a) The total (top panel) and atom-resolved projected DOSs of the Au adsorbed on the bridge site, the latter of which are rescaled so that characteristic features can be seen more clearly. The Ce and O atoms in the PDOS refer to the reduced Ce (i.e., Ce_i) and the O between Ce_i and the Au atom, respectively: (b) The three-dimensional contour plot of the spin density [dark areas around atoms (i.e., those at Ce_i)] of the system. For clarity, results from the (3×5) cell are shown.

adsorption structures is unaffected by the surface cell expansion, as will be shown later. Table I also shows that the Au adsorption at either the top or the bridge site leads to significant geometrical changes of the underlying O and the adjacent Ce atoms: Compared to those on the clean surface (O–Ce bond length: 2.37 Å), the O–Ce bonds become significantly longer. On the other hand, the O–Ce distances have little change for the hollow site adsorption.

To understand the energy and geometry differences of different adsorption modes, we next consider the electronic structures (mainly the top and the bridge site adsorption).

1. Top site

The Au adsorption on the top site was examined by Liu *et al.*[7] The main change of the electronic structures upon the adsorption was found to be the occupation of the original empty f state of a Ce atom. This was explained as follows: as Au starts to develop bonding with a surface O, which had the fully occupied $2p$ states on the clean surface, the electrons would evolve into the Au–O antibonding states, which could then tunnel into the neighboring empty f state. We plot in Fig. 3 the total and atom-resolved projected DOSs of both α and β spins for the Au adsorbed on the top site. Compared to the DOS of the clean surface, new states can be seen at just below E_F. From the projected DOS, these newly emerged states have predominant contributions from the f states of Ce atom (labeled as Ce_{ii}), which is neighboring the Au–O bond, and very small contributions from the O $2p$-s,d(Au) antibonding states. Note that these new states only appear in spin α. To find out where the net spin resides, we therefore plot the spin density, defined as the density difference between spins α and β, in Fig. 3(b) where the result from the large (3×5) cell is shown for best viewing [the result from the (2×2) cell is very similar]. It can be seen that the net spin (blue area) is located mainly at Ce_{ii}, with small densities at the Au atom. Considering the original $6s$ electron of the Au, the spin density plot clearly suggests that Au is oxidized: with respect to the neutral Au atom, Au is now positively charged ($+0.17e$ from the Bader charge calculation, which is a widely used method for charge analysis[26]). Another salient feature of the DOS is the significant shift of the original O $2p$ states toward lower energies, e.g., the small densities of states at around -5.5 eV, due to the formation of the O $2p$-d(Au) bonding. Compared to that of the clean surface, the band center of the original O $2p$ is lowered by 0.54 eV. These electronic features are consistent with the previous study. A minor difference exists in the shape of the occupied f orbital. Despite the nominal orbital degeneracy, the electrons here prefer the occupation of the f orbital with the magnetic quantum number $m_l=2$ [Fig. 3(b)] instead of $m_l=1$ shown in the previous work.[7] The energy difference between the two states is, however, likely to prove negligible, so we should probably not invest this point with great importance.

Returning to the adsorption geometry, because the partially filled f states are located at Ce_{ii}, Ce_{ii} has the largest displacement from its original position and consequently the longest distance to the O (Table I). It should be mentioned that we have also tried to assign the initial spin on Ce atoms that are not neighboring the Au–O bond, and we have found that the spin after optimization was always relocated to the Ce that is neighboring the Au–O bond in our calculations.

2. Bridge site

Considering next the DOS of Au on the most stable bridge site (shown in Fig. 4), we also find the occupation of the original empty f state. However, the filled f states are ~0.2 eV lower in energy than that in the DOS of Au on the

top site. By examining the spin density, we find that the *f* electron does not locate at the nearest (Ce_{iii}) or the next-nearest Ce (Ce_{ii} and Ce_{iv}) of the Au, but at a further Ce atom (Ce_i) which is also a neighbor of an O–Au bond [see the labeling convention in Fig. 2(b) or Fig. 4(b)]. This is because Ce_{ii}, Ce_{iii}, and Ce_{iv} have relatively short distances with the Au (3.35, 2.87, and 3.35 Å), and significant Coulomb repulsion would arise if the spin were to reside on any of these Ce atoms. Indeed, when we assigned the initial spin on Ce atoms other than Ce_i, we found that the spin would move to Ce_i in our calculations. These electronic features are also reflected in the geometrical changes caused by the adsorption: in Table I, Ce_i with the partially filled *f* states is the furthest Ce atom away from O_s; the $Ce_{iii}-O_s$ bond also has a long distance because Ce_{iii} is the closest Ce atom to the Au. In addition to the occupation of the *f* states, we also observe a significant downward shift of the original O 2*p* states, owing to the O 2*p*-*d*(Au) bonding formation. Despite the small DOS appearing at relatively high energies (i.e., those at around −1.0 eV), which are also induced by the O 2*p*-*d*(Au) bonding, the band center of the whole O 2*p*-*d*(Au) bonding states is 0.16 eV lower than that found for Au on the top site, indicating the overall stronger bonding for Au on the bridge site. These results can be understood from the atom-resolved projected density of state (PDOS) in Figs. 3(a) and 4(a). When Au adsorbs on the top site, small parts of its *d* states appear at low energies, most notably those around −5.5 eV, which can be ascribed to the bonding with O along the bond axis (i.e., perpendicular to the surface plane), whereas the other *d* states largely remain at relatively high energies (e.g., −3 to −2 eV), without significant overlap with the O 2*p* states. On the other hand, when Au adsorbs on the bridge site, large parts of its *d* states appear at low energies ranging from −5 to −3 eV, which can be ascribed to the broad O 2*p*-*d*(Au) overlap owing to the three centered O–Au–O bonding along the Au–O bond axes, whereas only relatively small parts of the *d* states appear at high energies. Therefore, although the Au–O bonding with the Au on the top site is strong, consistent with the lowest energy bonding states (−5.5 eV) and also justified from the short Au–O distance, the broader overlap of O 2*p*-*d*(Au) states make the overall Au–O bonds stronger when Au is on the bridge site. Furthermore, we note that compared to the case of Au on the top site, negligible spin densities are observed at Au on the bridge site, suggesting that the Au adatom is oxidized to a larger degree. Indeed, we find that the Au charge is now +0.32*e*, which is significantly more positive than when adsorbed on the top site. Last, unlike the DOS of Au on the top site, there are no O 2*p*-*s*,*d*(Au) antibonding states just below E_F in the DOS of the Au on the bridge site. This feature can be ascribed to the fact that more charge has been transferred from Au to Ce when Au adsorbs on the bridge site, so that the antibonding states are unoccupied.

It is worth noting that among the four surface O atoms on the (2×2) surface, half of them would directly bind with the Au adatom upon bridge site adsorption. In a larger cell, a lower percentage of O atoms is involved in the bonding with Au, which suggests that more O 2*p* states would not be affected significantly by the adsorption and that the band center of the whole O 2*p* states would be higher than that in the (2×2) cell. Therefore, a somewhat weaker Au–O bond is expected at lower coverages of Au. On the other hand, one may also expect a somewhat stronger Au–O bond because of the decrease of the repulsion between unit cells at lower coverages of Au. To examine the coverage dependence, we have therefore carried out calculations for Au adsorption on the top and bridge sites in a large (3×5) cell. From the results listed in parentheses in Table I, adsorption at the top site becomes ~0.05 eV stronger, suggesting that the effect from the decrease of the repulsion in the large cell prevails so that the overall result is the slightly enhanced Au–O bond. On the other hand, the adsorption at the bridge site becomes ~0.03 eV weaker, suggesting that the effect from the decrease of the repulsion is strongly offset by that from the lesser involvement of surface O atoms in the Au–O bonding so that the overall result is the slightly weakened bond. Despite the coverage dependence of the adsorption energies, the bridge site is still more favorable than the top site. We should mention that in real catalysts, Au–Au interaction would also affect adsorption energies. We expect that the Au–Au repulsion would reduce or moderate the interaction of Au with the surface, so that the bonding strength and the charge transfer may not be as significant as in the case of a single Au atom.

3. Hollow site

The finding that hollow sites are the least favorable is not surprising, because of the long Au–O distances in the adsorption geometry. When Au is deposited on a hollow site, it is not possible to achieve similar Au–O distances to those in the top or bridge site adsorptions: for example, if the distances between Au and adjacent surface O atoms were ~2.4 Å, the distances between the Au and the adjacent Ce atoms would become ~2.6 Å, which are apparently too short to achieve. Due to the long Au–O distances, the O 2*p*-*d*(Au) bonding is weak; the spin mainly resides at the Au (i.e., it remains essentially Au^0), and the occupancy of the *f* state is negligible.

B. Au at the O vacancy site

The most stable site for Au adsorption on the reduced surface is found to be close to the vacancy position: Au sits ~1.3 Å above the surface (with respect to the surface O atoms) and Au–Ce distances are ~3.2 Å. Considering the electronic structure, we show in Fig. 5 the DOS of the adsorption system. It can be seen that the *d*(Au) states are narrow; both α and β spins of *s*(Au) appear below E_F, the filled *f* states are only populated on a single Ce atom instead of two on the original reduced surface. From these features, the bonding picture of Au on the vacancy site is that no significant bonding or antibonding states form, because of the long distance between the Au and the surrounding O atoms (>3.5 Å); instead, some of the electrons in the *f* orbitals, which were localized at two Ce ions due to the removal of an O atom, would enter into the *s*(Au) orbitals. Therefore, in contrast to the role of the *f* states in the adsorption on the perfect surface, the *f* states on the reduced surface

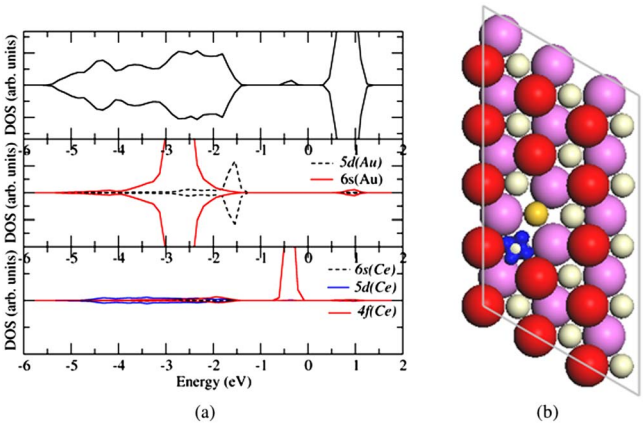

FIG. 5. (Color online) (a) The total (top panel) and atom-resolved projected DOSs of the Au adsorbed near the O vacancy, the latter of which are rescaled so that characteristic features can be seen more clearly. The Ce atom in the PDOS is the reduced Ce: (b) The three-dimensional contour plot of the spin density [dark areas around atoms (i.e., those at a Ce ion)] of the system. For clarity, results from the (3×5) cell are shown.

act as electron donor instead of electron acceptor. Clearly, the pairing of s(Au) electrons is mainly responsible for lowering the energy of the adsorption system. Moreover, strong ionic bonding character develops between the Au and the surrounding Ce atoms, since Au is now significantly negatively charged ($-0.62e$ from the Bader analysis). It is interesting to note that the remaining Ce^{3+} ion is neighboring $Au^{\delta-}$, with a distance of 3.2 Å, whereas it is impossible to achieve such a distance between Ce^{3+} and $Au^{\delta+}$ (as shown earlier), which also suggests the attractive interaction in the former. It should be mentioned that other arrangements with the initial spin placed on Ce atoms other than those neighboring the Au always revert, in our calculations, to the situation depicted in Fig. 5.

The bridge and top sites (the two most favorable sites on the perfect surface) are much less favorable than the vacancy site: the adsorption energies of Au being at the bridge site and the top site are −1.20 and −1.01 eV, respectively, which are similar to the corresponding energies on the perfect surface. This is because the vacancy is not directly involved in the bond formation in these two cases and thus plays an insignificant role. The local electronic features of those two cases are also similar to those on the perfect surface and thus are not discussed further here. It is interesting to note that these adsorptions can be also viewed as O vacancy formation at the stoichiometric surface where Au is preadsorbed and thus, one can examine if the preadsorbed Au facilitates the O vacancy formation or not. Since the Au adsorption energies in these cases are similar to those at the pure stoichiometric surface, the O vacancy formation energies are also similar to that from the pure stoichiometric surface, i.e., the preadsorbed Au has almost no influence on the O vacancy formation. We note that this result is different from the O vacancy formation on the {110} and {100} surfaces, where the preadsorbed Au facilitates the O vacancy formation.[27] Considering different geometries of those two surfaces from the {111} surface, the Au adsorption geometries and electronic structures would also be different and thus the different O vacancy formation is not surprising.

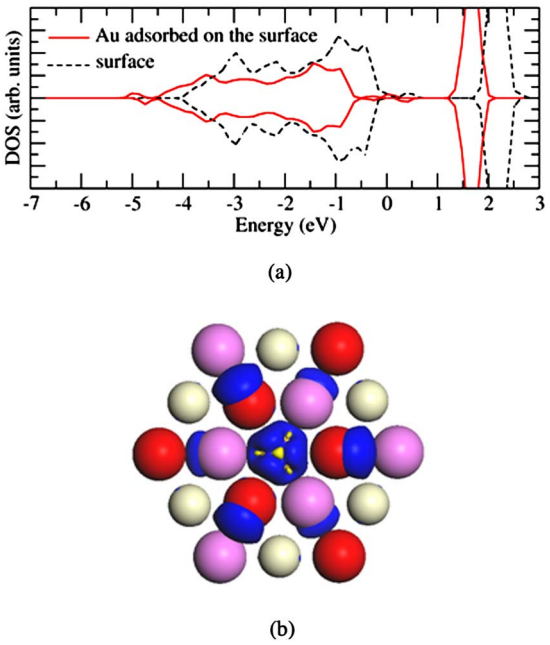

FIG. 6. (Color online) (a) The total DOS of Au adsorbed near the Ce vacancy: (b) The three-dimensional contour plot of the spin density [dark areas around atoms (i.e., those at O and Au ions)] of the system. For best viewing of the spin density, the atomic radii are drawn differently from previous pictures. Note that in addition to the six O atoms adjacent to the Au, the O beneath the Au (not visible) also has net spin.

C. Au at the Ce vacancy

There are suggestions in the literature that adsorption of Au at a Ce vacancy site substantially increases the adsorption energy.[4,9] Our calculations show no different results from the previous suggestion: with respect to the defective surface with a Ce vacancy, the Au adsorption energy is −5.94 eV in a (2×2) cell, which is much larger than the adsorption energies calculated on the stoichiometric and reduced surfaces. However, we consider that the much larger adsorption energy is owing to the much lower stability of the surface with Ce vacancies.

Because of the removal of a Ce atom (the electron donor in ceria), the negative charges of those O atoms adjacent to the defect decrease significantly: among seven such O atoms, the three surface O and the four subsurface O atoms have charges, respectively, $\sim0.4e$ and $\sim0.3e$ less negative than the corresponding atoms on the perfect surface, indicating significant weakening of the ionic bonding in the system. The bond weakening can be also seen from the DOS of the defective surface with the Ce vacancy, shown in Fig. 6 (the dashed curve). Compared to that of the perfect or the reduced surface, the O $2p$ states move considerably toward higher energies, suggesting that the surface with the Ce vacancy could be much less stable. Upon Au adsorption at the Ce vacancy, the $2p$ states lower their energies significantly (the red curve). This is largely because the charge losses of the seven O atoms adjacent to the original defect are compensated to a certain degree by the contribution from the Au adatom (i.e., the ionic bonding is enhanced). However, the charges of these seven O atoms are not fully recovered: the three surface O and the four subsurface O atoms still possess

TABLE II. Au adsorption energies (ΔE_a) on the stoichiometric surface (denoted as "Stoi"), the surface with an O vacancy (denoted as "O vacancy"), and the surface with a Ce vacancy (denoted as "Ce vacancy"), and vacancy formation energy (ΔE_v) and the new Au adsorption energies (ΔE_a) when ΔE_v is also considered. The unit for these energies is in eV. Results from Ref. 9 are written in parentheses.

	Stoi	O vacancy			Ce vacancy		
	ΔE_a	ΔE_a	ΔE_a	ΔE_a	ΔE_a	ΔE_a	ΔE_a
2×2 cell	−1.17	−2.75 (−2.58)	2.67	−0.07	−5.94 (−5.65)	4.99	−0.95
3×5 cell	−1.14	−2.42	2.26	−0.16	−5.88	4.85	−1.02

charges, respectively, $\sim 0.2e$ and $\sim 0.1e$ less negative than those on the perfect surface. Therefore, net spins on these O atoms exist, as can be seen from the spin density plot in Fig. 6(b). Moreover, the Au adatom has a charge of $+1.23e$, much more than found on other surfaces.

IV. DISCUSSION

A. Implications in catalysis

We believe that the current study of a single Au atom on various surfaces is an important step toward understanding of the boundary structure between Au clusters and the ceria support, which in turn would hold promise to unravel their catalytic roles in the WGS reaction. Experimentally, Au clusters are thought to embed into the ceria lattice.[2] One important question concerning the boundary structure is therefore the anchoring site of the Au cluster: in essence, where does the first Au atom locate? Having calculated the energetics of Au adsorption obtained at various surface sites, we can provide some insight toward this issue.

In the last sections, the adsorption energies (ΔE_a) for Au on surfaces with vacancies are calculated with respect to the surfaces with the vacancies already created, in order to make comparison with previous studies.[4,7,9] We note that values from ΔE_a could be misleading in interpreting the stability of Au adsorption on various surfaces, because one must consider how the adsorption energy varies when taking the vacancy formation into account. To this end, we define the vacancy formation energy (ΔE_v) as

$$\Delta E_a = E_{\text{surf}} - E_{\text{stoi}} + \tfrac{1}{2}N_{\text{O-}}E_{\text{O}_2} + N_{\text{Ce-}}(g^{\text{bulk}}_{\text{CeO}_2} - E_{\text{O}_2}) \qquad (2)$$

and the new adsorption energies ($\Delta E'_a$), with ΔE_v being taken into account, as

$$\Delta E^1_a = E^{\text{Au}}_{\text{surf}} - E_{\text{stoi}} + \tfrac{1}{2}N_{\text{O-}}E_{\text{O}_2} + N_{\text{Ce-}}(g^{\text{bulk}}_{\text{CeO}_2} - E_{\text{O}_2}) - E_{\text{Au}}, \qquad (3)$$

where $g^{\text{bulk}}_{\text{CeO}_2}$ and ΔE_{O_2} are the energies of a formula unit of the bulk and of an O_2 molecule, respectively, $N_{\text{O-}}$ and $N_{\text{Ce-}}$ are the numbers of Ce and O vacancies, respectively, and the rest of the terms are self-explanatory. In fact, Eq. (3) is the sum of Eqs. (1) and (2).

Table II summarizes ΔE_a, ΔE_v, and $\Delta E'_a$. It can be seen that while Au possesses largest ΔE_a when it adsorbs at the Ce vacancy site, ΔE_v for the Ce vacancy formation is also very large. The offsetting between ΔE_a and ΔE_v generates some interesting results: while Au still prefers the Ce vacancy site to the O vacancy site, Au adsorption on the perfect surface appears to be the most stable. Of course, we note that to illustrate the stability of a system, especially in equilibrium with a given environment, one must also consider the thermodynamic behavior of the system. Thus, a comprehensive *ab initio* thermodynamic analysis is currently under way, in the hope of resolving this issue.

B. Comparisons with previous studies using different methodologies

We note that in studying Au/CeO_2 systems, some previous calculations used the standard DFT,[4] which is well known to fail the description of reduced ceria system such as bulk Ce_2O_3 and the reduced CeO_2 surfaces.[28] Thus, we exclude comparison with the results reported in Ref. 4, which are likely to be incorrect. Results from a DFT+U calculation by Chen *et al.*[9] are listed in Table II (brackets), which agree with the corresponding data obtained in the current work, although we disagree with the conclusion from Ref. 9 that DFT and DFT+U give similar understanding of chemical issues.

We mainly compare here our results with the study in Ref. 7, which is not a standard DFT calculation in the sense that it achieved the correct localization features of f electrons by modifying the density-mixing scheme in the calculations. Since the results from standard DFT are not trustworthy, this comparison provides a unique opportunity for us to examine the energy effect from the U term. We first consider Au adsorption on the stoichiometric surface. For the top site adsorption (the bridge site was overlooked in Ref. 7), the energy previously reported [−1.26 eV in a (2×2) cell (Ref. 7)] is more negative than that obtained in the present work (−0.96 eV). Disregarding the effects such as cutoff energy and k-points, we interpret the discrepancy as follows. In principle, the U term in the DFT+U method introduces an on-site Coulomb repulsion term, which promotes the f electron localization. As a result, energies of relevant systems would be increased. The inclusion of the U term in DFT calculations would have more significant effects on the Au adsorption system than on the clean surface, since the f orbitals are partially filled in the former. On the reduced surface, we find that the adsorption energy (−2.75 eV in a 2×2 cell) calculated in the present work is much more negative than the previously reported value (−1.86 eV in a 2×2 cell).[7] Interestingly, this result appears to be in sharp contrast to the opposite effect of the U term on the adsorption energy on the stoichiometric surface. However, we consider that on the re-

duced surface, the adsorption system has fewer filled f orbitals (one Ce^{3+} ion) than the pure defective surface does (two Ce^{3+} ions). Thus, by including the U term, the total energy of the adsorption system increases to a lesser extent than that of the pure reduced surface, and consequently the adsorption energy becomes more negative. Finally, we should mention that it is difficult to judge the accuracy of the two sets of adsorption energies from the two methods, because of the lack of experimental data. Both the method used in Ref. 7 and the DFT+U approach are rather empirical: the mixing scheme needs to be changed in the former and the U parameter needs to be changed in the latter, in order to have a satisfactory agreement with known experimental data. Nonetheless, we expect that the comparison made here would pose a challenge on the performance of DFT+U for predicting energetics at ceria surfaces, which is known to be not always satisfactory.[28]

V. CONCLUSION

The present work has undertaken a systematic investigation of Au adsorption on various ceria surfaces. Discrepancies with previous studies have been found and clarified, including the adsorption sites and the adsorption energetics. In the absence of direct experimental data for comparison, we mainly resort to electronic analysis to rationalize our results. We show that the Ce 4f states play a pivotal role in the Au adsorption on the stoichiometric and the reduced surfaces. In the former, the original empty nonbonding f states, lying just above the Fermi level, act as an electron acceptor, so as to stabilize the adsorbed Au; in the latter, the partially occupied f states due to the removal of O atoms, lying just below the Fermi level, act as an electron donor, also being able to stabilize the adsorbed Au. We also show that when Au adsorbs at the Ce vacancy site, the adsorption, with the Ce vacancy formation energy being taken into account, is slightly weaker than the adsorption at the stoichiometric surface.

ACKNOWLEDGMENTS

We acknowledge the Cambridge Isaac Newton Trust (C.Z.) and The Royal Society (S.J.J). A.M. is supported by the EURYI scheme (see www.esf.org/euryi).

[1] Q. Fu, H. Saltsburg, and M. Flytzani-Stephanopoulos, Science **301**, 935 (2003).
[2] R. Burch, Phys. Chem. Chem. Phys. **8**, 5483 (2006).
[3] F. Boccuzzi, A. Chiorino, M. Manzoli, D. Andreeva, and T. Tabakova, J. Catal. **188**, 176 (1999).
[4] D. Tibiletti, A. Amieiro-Fonseca, R. Burch, Y. Chen, J. M. Fisher, A. Goguet, C. Hardcare, P. Hu, and D. Thompsett, J. Phys. Chem. B **109**, 22553 (2005).
[5] J. A. Rodriguez, M. Pérez, J. Evans, G. Liu, and J. Hrbek, J. Chem. Phys. **122**, 241101 (2005).
[6] X. Wang, J. A. Rodriguez, J. C. Hanson, M. Pérez, and J. Evans, J. Chem. Phys. **123**, 221101 (2005).
[7] Z. Liu, S. J. Jenkins, and D. A. King, Phys. Rev. Lett. **94**, 196102 (2005).
[8] V. Shapovalov and H. Metiu, J. Catal. **245**, 205 (2007).
[9] Y. Chen, P. Hu, M.-H. Lee, and H. Wang, Surf. Sci. **602**, 1736 (2008).
[10] S. Fabris, S. de Gironcoli, S. Baroni, G. Vicario, and G. Balducci, Phys. Rev. B **71**, 041102 (2005).
[11] S. Fabris, G. Vicario, G. Balducci, S. de Gironcoli, and S. Baroni, J. Phys. Chem. B **109**, 22860 (2005).
[12] G. Kresse, P. Blaha, J. L. F. Da Silva, and M. V. Ganduglia-Pirovano, Phys. Rev. B **72**, 237101 (2005).
[13] C. Loschen, J. Carrasco, K. M. Neyman, and F. Illas, Phys. Rev. B **75**, 035115 (2007).
[14] G. Kresse and J. Furthmuller, Phys. Rev. B **54**, 11169 (1996); G. Kresse and J. Hafner, *ibid.* **48**, 13115 (1993); J. Phys.: Condens. Matter **6**, 8245 (1994).
[15] V. I. Anisimov, J. Zaanen, and O. K. Andersen, Phys. Rev. B **44**, 943 (1991).
[16] A. Rohrbach, J. Hafner, and G. Kresse, J. Phys.: Condens. Matter **15**, 979 (2003).
[17] A. I. Liechtenstein, V. I. Anisimov, and J. Zaanen, Phys. Rev. B **52**, R5467 (1995).
[18] S. L. Dudarev, G. A. Botton, S. Y. Savrasov, C. J. Humphreys, and A. P. Sutton, Phys. Rev. B **57**, 1505 (1998).
[19] M. Nolan, S. Grigoleit, D. C. Sayle, S. C. Parker, and G. W. Watson, Surf. Sci. **576**, 217 (2005).
[20] C. W. M. Castleton, J. Kullgren, and K. Hermansson, J. Chem. Phys. **127**, 244704 (2007).
[21] J. L. F. Da Silva, M. V. Ganduglia-Pirovano, J. Sauer, V. Bayer, and G. Kresse, Phys. Rev. B **75**, 045121 (2007).
[22] J. P. Perdew and A. Zunger, Phys. Rev. B **23**, 5048 (1981).
[23] S. H. Vosko, L. Wilk, and M. Nusair, Can. J. Phys. **58**, 1200 (1980).
[24] J. P. Perdew, J. A. Chevary, S. H. Vosko, K. A. Jackson, M. R. Pederson, D. J. Singh, and C. Fiolhais, Phys. Rev. B **46**, 6671 (1992).
[25] G. Kresse and D. Joubert, Phys. Rev. B **59**, 1758 (1999).
[26] R. F. W. Bader, *Atoms in Molecules: A Quantum Theory* (Oxford University, New York, 1990).
[27] M. Nolan, V. S. Verdugo, and H. Metiu, Surf. Sci. **602**, 2734 (2008).
[28] M. V. Ganduglia-Pirovano, A. Hofmann, and J. Sauer, Surf. Sci. Rep. **62**, 219 (2007).